THE JOURNAL OF PHYSICAL CHEMISTRY B

Article

pubs.acs.org/JPCB

Anomalous Volume Phase Transition Temperature of Thermosensitive Semi-Interpenetrating Polymer Network Microgel Suspension by Dielectric Spectroscopy

Man Yang and Kongshuang Zhao*

College of Chemistry, Beijing Normal University, Beijing 100875, China

ABSTRACT: A new experimental result from dielectric spectroscopy of poly(*N*-isopropylacrylamide)/poly(acrylic acid) semi-interpenetrating polymer network (PNIPAM/PAA SIPN) microgel, which undergoes significant volume phase transition, is reported. Two significant dielectric relaxations were observed around 0.1−0.5 MHz and 1−5 MHz, respectively. The high-frequency relaxation is attributed to the migration of counterions tangentially and radially along the domain formed by linear PAA chains (counterion polarization). The temperature dependence of the domain size obtained from this relaxation shows that the SIPN microgel with higher content of PAA has better thermal response and swelling property. The low-frequency relaxation shows two separate mechanisms below and above the volume phase transition temperature (VPTT), which are dominated by different relaxation processes, respectively: micro-Brownian movement of solvated side groups of PNIPAM dominates when T < VPTT, while the interfacial polarization does when T > VPTT. A dielectric model was proposed to describe the collapsed microspheres suspension, from which the electrical parameters of microgel were calculated. The permittivity of microgel shows that a special ordered arrangement of water molecules is formed in microgel with less PAA. Thermodynamic parameters obtained from Eyring equation reveal that the difference in PAA content has a great influence on the thermodynamics of the phase transition process. Besides, it was found that the VPTT of the SIPN microgel was significantly increased compared with pure PNIPAM hydrogel microspheres. The essence of anomalous VPTT revealed by relaxation mechanism is the difference in composition content leading to different hydrophilic/hydrophobic and electrostatic interaction. Determining the reason for anomalous VPTT is of instructive significance to understand the volume phase transition of complex polymer materials.

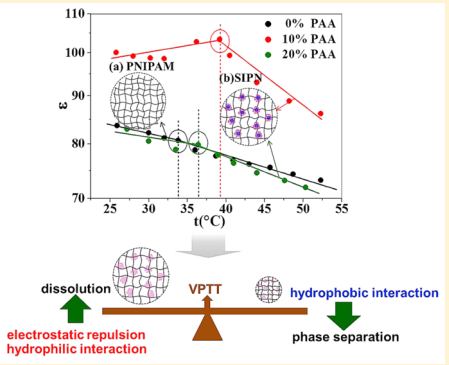

1. INTRODUCTION

In recent years, thermosensitive microgels have been increasingly used in fluorescence probe,[1] drug controlled release,[2,3] sensor,[4] and cell capture and release.[5] Such thermosensitive materials usually contain typical polymer poly(*N*-isopropylacrylamide) (PNIPAM), for instance, poly(*N*-isopropylacrylamide-*co*-acrylamide) hydrogel with silica−gold nanoshells[2] and ABC triblock polymer poly-[(propylene-sulde)-*block*-(*N*,*N*-dimethylacrylamide)-*block*-(*N*-iso-propylacrylamide)] (PPS-*b*-PDMA-*b*-PNIPAAM)[3] that forms physically cross-linked hydrogels above volume phase transition temperature (VPTT). In practical applications, the former hydrogel is designed to have a VPTT above physiologic temperature, so that there is a near absence of drug release during the transport of drug, but there is controlled drug release on arrival at the targeted cells.[2] VPTT of the latter needs to be lower than physiological temperature; otherwise, the ABC triblock polymer cannot become a stable hydrogel in vivo and be used as drug carrier.[3] Research shows that the accurate confirmation and regulation of VPTT is the key to their successful application. The adjustment of VPTT can be achieved by introducing a hydrophilic/hydrophobic network or chain to the PNIPAM network to form an interpenetrating or semi-interpenetrating polymer network (IPN or SIPN).[6]

It is known to all that volume phase transition of PNIPAM is related to the competition between the hydrophobic interactions of isopropyl in side chains as well as that of the backbone and the hydrogen-bond interactions of amide group and water.[7] However, when another polymer is introduced into the PNIPAM network, the interactions in (S)IPN become complex. It contains interactions between not only PNIPAM and solvent (H-bond and hydrophobic interaction), but also PNIPAM and other polymer chains (H-bond, electrostatic interaction, etc.),[7] making the relation between the content of doped polymer and VPTT ambiguous and complicated. Liu et al.[8,9] prepared pH/temperature dual stimuli-responsive nanogels with IPN structure composed of PNIPAM and PAA networks. The dynamic laser light scattering (DLLS) results indicated that the volume phase transition temperature of IPN nanogels and PNIPAM nanogels are identical. Hu[10−12] also synthesized temperature and pH dual response PNIPAM/PAA IPN microgels with the same VPTT as PNIPAM microgels. The study of Stile et al.[13] suggested that the PAA chains in the PNIPAM-based/PAA SIPN do not significantly affect the

Received: June 9, 2015
Revised: September 19, 2015
Published: September 24, 2015

DOI: 10.1021/acs.jpcb.5b05491
J. Phys. Chem. B 2015, 119, 13198−13207

VPTT of the semi-IPNs, but the injectability and transparency as well as the phase transition. Other studies considered the introduction of the second network to have an effect on the VPTT of PNIPAM. For example, Kozhunova et al.[14] studied the conversion, swelling ratio, and swelling/shrinking kinetics of thermosensitive ionic SIPN based on PNIPAM and poly(styrene sulfonic acid sodium salt) (PSS) at different PSS fractions and molecular weight. The results show that swelling behavior and VPTT of the SIPN are controlled by the fraction of the polyelectrolyte PSS and the increase in charged polyelectrolyte unit leads to a slight increase of VPTT. Zhang et al.[15,16] synthesized poly(*N*-isopropylacrylamide)/poly(2-hydroxyethyl methacrylate) (PNIPAM/PHEMA) IPN microgel for the first time. By means of IR spectroscopy in combination with the perturbation correlation moving window (PCMW) technique and two-dimensional correlation spectroscopy (2Dcos) analysis, they found that due to the hydrophobic and non-thermoresponsive properties of PHEMA and the special IPN structure, the VPTT of the IPN microgel exhibits a decreasing trend. The above research shows that whether another network will affect the VPTT of a temperature-sensitive network is still controversial, which will undoubtedly hinder the rational optimization of (S)IPN materials.

So far, the volume phase transition of interpenetration of (S)IPN microgel has been studied by many methods or techniques experimentally. The rheological methods[10] can provide information such as the molecular weight, distribution, and gelation temperature of the microgel systems. By using microscopy techniques,[9] one can directly observe the micro or nanostructure, but one generally needs to dry the sample; thus, the images shown are not "as is" as in aqueous solution. Conventional diffraction techniques small angle neutron scattering (SANS)[17] used to study the super structure formed by fiber in the gel need sophisticated mathematical analysis to obtain information. In addition to these, a variety of spectroscopic techniques, such as nuclear magnetic resonance spectroscopy (NMR)[18] and infrared spectroscopy (IR),[19,20] have been widely used to characterize the gel system and to provide information about the molecular structure of the gel.

Dielectric spectroscopy, which can measure the internal dipole and fluctuation of interface charge inside substances, has been increasingly used in the study of smart gels. Ono et al.[21,22] investigated the hydration and molecular dynamics of linear PNIPAM chains in temperature-changing process in the frequency range 10^7-10^{11}Hz and determined the number of hydrated water molecules per *N*-isopropylacrylamide and its change as temperature increases. Nakano et al.[23] studied dielectric relaxation behavior of linear PNIPAM in protic and aprotic solvents in the same microwave frequency range and pointed out that the molecular dynamics of PNIPAM chains is associated with the hydrogen bonding between PNIPAM chains and solvent molecules. In radiofrequency Marieke Füllbrandt and his co-workers[24,25] monitored the volume phase transition of PNIPAM microgel with different cross-linking density and the "coil-to-globule" of linear PNIPAM by both the frequency and the temperature dependence of the conductivity spectra. Meanwhile, they[26] also studied the molecular dynamics of linear PNIPAM with dependence on the concentration, temperature, and polymer chain length (molecular weight) in aqueous media in a frequency range from10^{-1} to 10^{11} Hz. If special attention is paid to the reorientation of water molecules, the suggestion of dehydration of the PNIPAM chains at the lower critical solution temperature was confirmed by calculating a dehydration number. Besides, an experimental device to simultaneously measure the light transmittance and dielectric properties of thermosensitive hydrogels was developed by Gómez-Galván,[27] from which the volume phase transition was monitored by measuring light transmittance, permittivity, and the dielectric loss tangent as a function of temperature. Zhou et al.[28] characterized PNIPAM microgel with different charge distribution and cross-linking density distribution by DLS and dielectric spectroscopy. In our recent work,[29] the volume phase transition behaviors of three types of PNIPAM microgel with different cross-linking density distribution and their dielectric properties were systematically analyzed, and the results revealed that the spatial distribution of the cross-linking density has almost no effect on the volume phase transition temperature. Obviously, most of these studies are focused on solution of pure PNIPAM microgel and PNIAPM linear chains; no research has addressed (S)IPN microgel suspension in which PNIPAM is involved. This is because the introduced polymer will produce interactions and the motion patterns of macromolecules and ions become much more complicated. Despite this difficulty, dielectric study of SIPN microgel suspension is undoubtedly necessary. One one hand, identification of the motion pattern and relaxation position of complex polymers is a persistent problem in polymer physics, so it is also an opportunity to explore different interactions among polymers which is ubiquitous throughout the application of polymers. On the other hand, awareness of the relationship between network components and VPTT is crucially significant to regulate VPTT so as to expand the application scope of temperature-sensitive microgel.

In the present work, measurements of SIPN microgel suspensions composed of typical thermosensitive PNIPAM and linear PAA under varying temperature were performed by dielectric spectroscopy for the first time. Two remarkable temperature dependent dielectric relaxations were observed. The relaxation mechanisms and the temperature dependence of the relaxation parameters are discussed in detail. In particular, we expect to obtain the effect of PAA content on VPTT of SIPN microgel as well as microscopic information about volume phase transition of SIPN microgel.

2. EXPERIMENTAL SECTION

2.1. Materials and Preparation of Sample. *Materials.*[30] *N*-Isopropylacrylamide (NIPAM) was purchased from Tokyo Chemical Industrial Co., Ltd. and recrystallized with *n*-hexane, then stored in brown bottles at 4 °C. *N,N,N′,N′*-Tetramethylethylene-diamine (TEMED), acrylic acid (AA), and *N,N′*-methylene-bis(acrylamide) (MBA) were purchased from Sinopharm Chemical Regent Beijing Co., Ltd. Span 80 was bought from Farco Chemical supplies, Beijing, China. Ammoniumpersulfate (APS) was supplied from Shantou Xilong Chemical Factory, Guangdong, China. Sodium hydroxide, sulfuric acid, and cyclohexane were bought from Beijing Chemical Works, China. All these reagents were in analytical grade and used as received. Deionized water used throughout the preparation process was produced by Rios-water system (Millipore Corp., America).

Sample Preparation. The PNIPAM/PAA SIPN microgels were fabricated with premix membrane emulsification technique.[31,32] In other words, NIPAM monomer and the linear PAA chains with cross-linking agent and initiator APS were commingled together with water as water phase. Cyclohexane

DOI: 10.1021/acs.jpcb.5b05491
J. Phys. Chem. B 2015, 119, 13198−13207

containing a certain amount of Span 80 was used as oil phase. The coarse emulsion prepared by mixing the oil phase and water with low speed stirring was extruded through the SPG membrane under a specific nitrogen pressure to get the final emulsion. Then, TEMED dissolving in cyclohexane was added into the emulsion to initiate the polymerization at 25 °C. After 4 h, the obtained microspheres were centrifuged and washed with acetone and water 3 times, separately. The obtained microspheres were dispersed in deionized water for further use. The pH values of SIPN microgel solution were 5.32 (10 wt % PAA) and 5.34 (20 wt % PAA), respectively. In this case PAA is deprotonated and the SIPN microgel is negatively charged. Because of the introduction of ammonium persulfate in the preparation process, the counterion in SIPN microgel solution is mainly NH_4^+.

For semi-interpenetrating network structure, although interpenetration can be realized by controlling the preparation process, the two networks in SIPN are actually phase-separated from the microscopic view and polymer II (linear PAA in this work) will form a domain in polymer I (PNIPAM network in this work).[33−35] The SIPN microgels are represented by the model shown in Figure 5.

2.2. Dielectric Measurements. Dielectric measurements were carried out using 4294A precision impedance analyzer (Agilent Technologies) over a frequency range from 40 Hz to 110 MHz and a temperature range between 25 and 55 °C. The applied alternating field was 500 mV. A dielectric measuring cell with concentrically cylindrical platinum electrodes (the effective area of the electrodes was 78.5 mm^2 and the electrode distance was 8 mm) was employed to load the samples. The temperature of the samples was controlled by a circulating thermostatic water jacket. The raw data, capacitance C_x and conductance G_x, measured at varying frequency was corrected according to the literature[36] and converted to the corresponding dielectric permittivity ε and conductivity κ through $\varepsilon = C_s/C_l$ and $\kappa = G_s\varepsilon_0/C_l$ (where $\varepsilon_0 = 8.8541 \times 10^{-12}$ F/m is the vacuum permittivity).

2.3. Determination of Relaxation Parameters. The complex permittivity of SIPN microgel suspension can be expressed as

$$\varepsilon^*(\omega) = \varepsilon(\omega) - j\varepsilon''(\omega) = \varepsilon(\omega) - j\frac{\kappa(\omega) - \kappa_l}{\omega\varepsilon_0} \quad (1)$$

where ε^* is complex permittivity, ε'' is dielectric loss. ω is angular frequency and $j = (-1)^{1/2}$. κ_l is low-frequency limit of conductivity, which was read out from the conductivity spectra at low frequency. When the ionic strength of the solution is larger, the electrode polarization (EP) will really affect the low-frequency relaxation, and affect its analysis. Many methods or technologies are used to correct EP effect. Serghei A. et al.[37] described a detailed analysis of dielectric data of EP based on charge transport mechanism at the ion−metal interface. To reduce and correct the EP effect that occurs in systems with higher conductivity, eq 2[38] with the EP term $A\omega^{-m}$ (where A and m are adjustable parameters) is used to fit dielectric data

$$\varepsilon^* = \varepsilon_h + \sum_g \frac{\Delta\varepsilon_g}{1 + (j\omega\tau_g)^{\beta_g}} + A\omega^{-m} \quad (2)$$

where ε_h is the high-frequency limit of permittivity, $\Delta\varepsilon_g$ and τ_g ($=1/(2\pi f_{0g})$, f_{0g} is characteristic relaxation frequency) indicate relaxation strength and relaxation time of the gth relaxation, respectively, and β_g ($0 < \beta_g \leq 1$) is the Cole−Cole parameter.

To determine the characteristic frequency of low-frequency relaxation which is masked by the EP effect, the derivative dielectric loss ε''_{der} is presented on the basis of the logarithmic derivative of raw ε as used by other researchers:[39−43]

$$\varepsilon''_{der}(\omega) = -\frac{\pi}{2}\frac{\partial\varepsilon}{\partial \ln\omega} \approx \varepsilon''_{true}(\omega) \quad (3)$$

By introducing the real part of eq 2 (i.e., the raw $\varepsilon(\omega)$) into eq 3, eq 4 is obtained:

$$\varepsilon''_{der}(\omega) = \frac{\pi}{2}\left(\sum_g \frac{\beta_g(\Delta\varepsilon_g)(\omega\tau_1)^{\beta_g}\cos\left[\frac{\beta_g\pi}{2} - (1+\beta_g)\theta_g\right]}{1 + 2(\omega\tau_g)^{\beta_g}\cos\frac{\beta_g\pi}{2} + (\omega\tau_g)^{2\beta g}}\right) + A\omega^{-m} \quad (4a)$$

and

$$\theta_i = \arctan\left[\frac{\sin(\beta_i\pi/2)}{(\omega\tau_i)^{\beta_i} + \cos(\beta_i\pi/2)}\right] \quad (4b)$$

The two equations have the same set of variables as those in eq 2 and can be used to fit the derivative dielectric loss spectrum.

As a representative case, the dielectric spectroscopy for the SIPN microgel suspension composed of PNIPAM and 10 wt % PAA at 36.2 °C were shown in Figure 1. Two distinct peaks

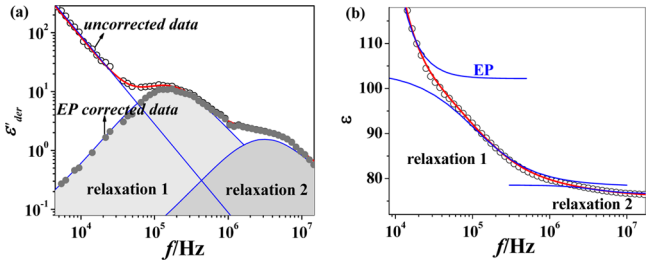

Figure 1. Derivative dielectric loss spectroscopy (a) and permittivity spectroscopy (b) for SIPN microgel composed of PNIPAM and 10 wt % PAA at 36.2 °C. The hollow and solid circles are the uncorrected raw data and corrected curves after subtraction of EP effect, respectively. The contributions of EP, relaxation 1 (low-frequency relaxation), and relaxation 2 (high-frequency relaxation) are represented by the blue solid line.

were observed in the derivative dielectric loss spectroscopy (Figure 1a). The hollow circles represent the raw derivative dielectric loss. The red solid line represents the best fitting curve, which is made of three parts (blue solid line): the EP effect and the contributions from relaxation 1 (low-frequency relaxation) and relaxation 2 (high-frequency relaxation), respectively. Simultaneously, two relaxations were found in the permittivity spectroscopy (Figure 1b). The best-fit relaxation parameters obtained according to the logarithmic derivative method were listed in Table 1.

In addition to the logarithmic derivative method, complex conductivity is also effective to deal with EP. Complex conductivity increment $\Delta\kappa^*$ relates with complex permittivity increment $\Delta\varepsilon^*$ by $\Delta\kappa^* = j\omega\varepsilon_0\Delta\varepsilon^*$; therefore

$$\Delta\kappa = \kappa - \kappa_l = \omega\varepsilon_0\Delta\varepsilon'' \quad (5a)$$

$$\Delta\kappa'' = \omega\varepsilon_0\Delta\varepsilon = \omega\varepsilon_0(\varepsilon - \varepsilon_h) \quad (5b)$$

DOI: 10.1021/acs.jpcb.5b05491
J. Phys. Chem. B 2015, 119, 13198−13207

Table 1. Relaxation Parameters of PNIPAM/PAA SIPN with 10 wt % PAA (a) and 20 wt % PAA (b) at Varying Temperatures

(a) t/ °C	τ_l/μs	τ_h/μs	$\Delta\varepsilon_1$	$\Delta\varepsilon_h$
25.8	1.41	0.094	5.9	4.6
28.0	1.38	0.077	7.7	3.9
30.2	1.35	0.062	9.4	3.8
33.8	1.25	0.051	12.4	2.3
36.2	1.09	0.042	20.9	2.0
39.2	8.47	0.039	23.4	1.5
40.5	7.73	0.037	22.1	1.5
44.0	6.29	0.032	17.7	1.4
48.2	5.51	0.031	15.2	0.9
52.3	4.59	0.029	12.9	0.8
(b) t/ °C	τ_l/μs	τ_h/μs	$\Delta\varepsilon_1$	$\Delta\varepsilon_h$
27.2	3.60	0.192	3.8	2.9
30.0	3.03	0.155	5.0	2.4
33.5	2.44	0.119	5.3	1.5
36.4	2.23	0.759	8.9	1.1
39.0	1.90	0.739	6.9	1.0
41.0	1.77	0.692	6.4	0.9
44.0	1.45	0.633	4.9	1.0
47.6	1.06	0.632	4.2	0.9
50.8	9.95	0.557	3.6	0.8

where ε_h is the limiting relative permittivity at high frequency, and can be accurately determined from the relative permittivity spectroscopy. According to eq 5, because EP usually occurs at a relative lower frequency range, the introduction of angular frequency ω into $\Delta\kappa^*$ can decrease the magnitude of EP and increase the magnitude of relaxations at higher frequency. By analysis of complex conductivity, the influence of EP can be reduced greatly. Figure 2 is a representative case for SIPN microgel suspension composed of PNIPAM and 10 wt % PAA at 36.2 °C. Similar to the logarithmic derivative method (Figure 1), two relaxations were observed and they were almost not affected by EP.

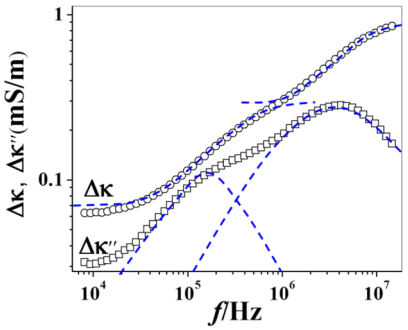

Figure 2. Complex conductivity spectroscopy for SIPN microgel composed of PNIPAM and 10 wt % PAA at 36.2 °C. The hollow circles and squares are real and imaginary parts of complex conductivity increasement, respectively.

The logarithmic derivative method and complex conductivity method are both effective to deal with EP. In this work, we use the logarithmic derivative method for further analysis.

3. RESULTS AND DISCUSSION

3.1. Dielectric Spectroscopy of SIPN Microgel Suspension. The temperature and frequency dependent logarithmic derivative loss ε''_{der} (Figure 3) show two relaxations with characteristic frequencies located at around 0.1−0.5 MHz and 1−5 MHz. ε''_{der} changes significantly in the vicinity of 39 and 36 °C for the two systems, respectively, indicating that both suspensions have undergone volume phase transition as illustrated in Figure 5, but at different temperatures, which depend on PAA content.

3.2. Low-Frequency Relaxation: Volume Phase Transition Process. Figure 4 shows the temperature dependence of the specific dielectric relaxation strength $\delta\varepsilon_l$ (defined as $\Delta\varepsilon_l/c$(c is the mass concentration of SIPN microgel) to eliminate the effect of particle concentration on the dielectric increment) of low-frequency relaxation for the two SIPN microgel solutions. The diametrically opposed changing trend of $\delta\varepsilon_l$ below and above VPTT suggests that the low-frequency relaxation process is dominated by different polarization mechanisms.

3.2.1. T < VPTT: micro-Brownian Motions. $\delta\varepsilon_l$ increases with temperature at T < VPTT. This means the low-frequency relaxation is irrelevant to the motion of the free counterions and dipole orientation polarization, because the dielectric increment decreases with temperature for these two mechanisms. Therefore, the low-frequency relaxation below VPTT is mainly caused by the micro-Brownian motions of side groups of PNIPAM. This process is closely associated with the H-bonding interactions, as confirmed by several researchers.[23,26,29] As illustrated in Figure 5, SIPN microgels are in highly swollen state (T < VPTT), and the hydrogen bonds between the amide groups and the water molecules (Scheme 1) are not favorable to the orientation movement of PNIPAM segments, resulting in relatively lower contribution of $\delta\varepsilon_l$ to the low frequency relaxation at lower temperatures. As temperature rises, part of the hydrogen bonds are opened, leading to the speeding up of random movement of side groups. Therefore, $\delta\varepsilon_l$ increases with temperature and shows a maximum when the temperature is near VPTT. When the temperature is raised above VPTT, the hydrogen bonds further fracture and the swollen gel loses water, and then the collapse occurs. Simultaneously, the micro-Brownian motions become more difficult because of the intramolecular hydrogen bond between the side chains of PNIPAM molecules.[7] As a result, $\delta\varepsilon_l$ decreases with temperature when T > VPTT. Note that in this temperature range, the SIPN microgel with higher content of PAA has the larger value of $\delta\varepsilon_l$ at the same temperature. This indicates that microgels with more PAA have relatively loose structure due to the larger electrostatic repulsion; as a result, the solvated side chains can move more freely within the space.

3.2.2. T > VPTT: Interfacial Polarization. Above VPTT, the PNIPAM network expels water and SIPN microgel collapses from a swollen microsphere to a compact one. In this process, a great deal of water molecules with high dielectric constant are expelled out, resulting in a decrease in the apparent permittivity of the compact particle and significant difference of dielectric constant between the collapsed microgel and aqueous solution. By this time, the SIPN microgel system can be regarded as a microsphere suspension which consists of microgel particles with volume fraction ϕ, permittivity ε_p, conductivity κ_p, and medium water with ε_w and κ_w, as shown in the right side of Figure 5. Therefore, the interfacial polarization plays a dominant role.

According to the interfacial polarization model of suspension,[44] the counterion migration distance can be characterized by the Debye length χ^{-1}, which is equivalent to the thickness of

DOI: 10.1021/acs.jpcb.5b05491
J. Phys. Chem. B 2015, 119, 13198−13207

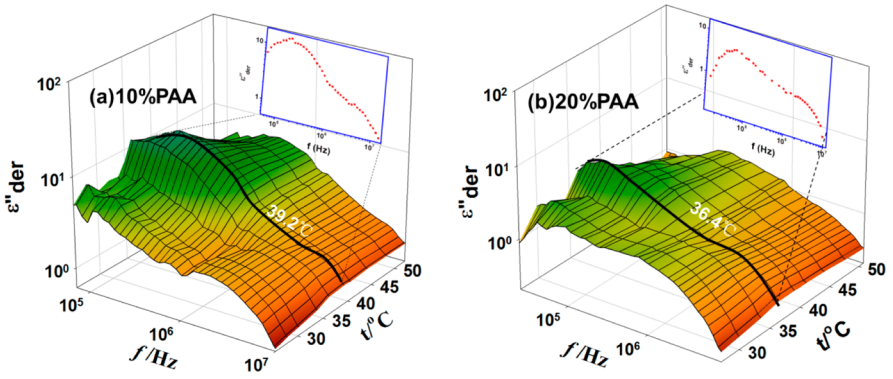

Figure 3. Logarithmic derivative loss ε''_{der} versus frequency and temperature in three-dimensional representations for SIPN microgel composed of different contents of PAA: (a) 10 wt %, (b) 20 wt %. The inset shows the dielectric loss spectrum at VPTT.

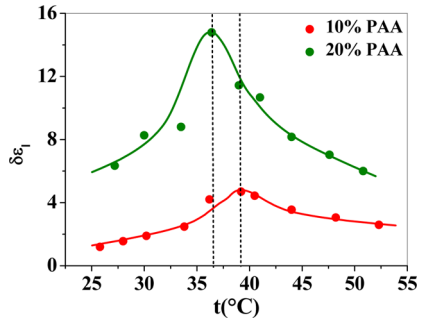

Figure 4. Temperature dependence of the specific low-frequency dielectric strength $\delta\varepsilon_l$.

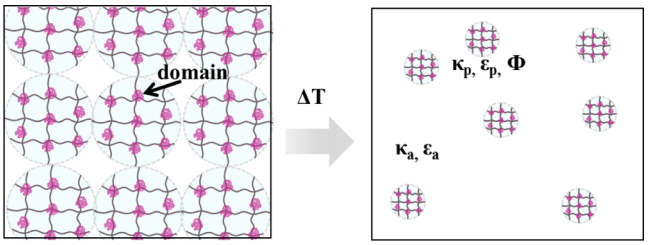

Figure 5. Schematic of SIPN microgel suspension during volume phase transition. The purple globule represents the domain formed by PAA. ε_a and κ_a are the permittivity and conductivity of water phase, respectively. ε_p, κ_p, and ϕ denote the permittivity, conductivity, and volume fraction of the collapsed microgel particles.

Scheme 1. Change of Hydrogen Bonds in PNIPAM Network As Temperature Rises

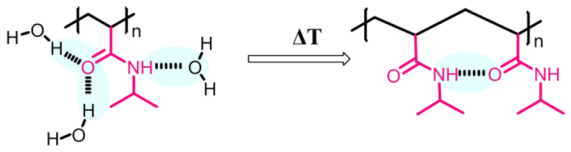

the electric double layer surrounding the microsphere and defined as

$$\chi^{-1} = \sqrt{\frac{\varepsilon_a \varepsilon_0 KT}{e^2 \sum_i C_i Z_i^2}} \tag{6}$$

where K and T are Boltzmann constant and absolute temperature; e, C, and Z are the elementary charge, the concentration, and the valence of the ion, respectively. ε_a is the permittivity of continuous medium in the suspension, as a function of temperature expressed as[45]

$$\varepsilon_a = 0.24921 \times 10^3 - 0.79069T + 0.72997 \times 10^{-3}T \tag{7}$$

The time necessary for the counterion to migrate the distance χ^{-1}, equivalently relaxation time τ_χ, is given by the equation[44]

$$\tau_\chi = \chi^{-2}/D_{NH_4^+} \tag{8}$$

where $D_{NH_4^+}$ is the diffusion coefficient of the counterion NH_4^+. By substituting $D_{NH_4^+}$ at each temperature ($D_{NH_4^+}$ is 1.957×10^{-5} cm^2/s at 25 °C and it increases by 2−3% per degree as the temperature increases)[45] and relaxation time τ_χ into eq 8, the obtained χ^{-1} varies between 55 and 79 nm (10 wt % PAA) and 80−120 nm (20 wt % PAA). The fluctuation is much smaller than the microsphere diameter. Meanwhile, χ^{-1} reduces as temperature increases and is in accordance with the trend of eq 6. This further proves that the low-frequency relaxation is caused by the interfacial polarization above VPTT. On the other hand, Figure 4 shows $\delta\varepsilon_l$ of the SIPN microgel that contains 20 wt % PAA is relatively large compared with that containing 10 wt % PAA. This is because of the different electrical properties of the two microgels at temperatures above VPTT ($(\varepsilon_a/\kappa_a - \varepsilon_p/\kappa_p)_{10\%PAA} \ll (\varepsilon_a/\kappa_a - \varepsilon_p/\kappa_p)_{20\%PAA}$).

3.2.3. Modeling Analysis of Collapsed SIPN Microgel Suspension. The phase parameters (ε_p, ε_w, κ_p, κ_w, ϕ) described in the microsphere suspension model are numerically calculated by the Hanai equation[46] described in the literature.[29,47−49] The results are shown in Table 2.

The temperature dependence of ε_p (Figure 6) shows an interesting result. Similarly, there are two inflections of ε_p at about 36 °C for 20% PAA and 39 °C for 10%, respectively. Besides, ε_p and ε_w have the following relationship: $\varepsilon_{p(10\%\ PAA)} > \varepsilon_w > \varepsilon_{p(20\%\ PAA)}$. It is generally known that the apparent permittivity of the SIPN microspheres can be expressed as[47]

$$\varepsilon_p = \varepsilon_w f_w + \varepsilon_{Polymer}(1 - f_w) \tag{9}$$

where ε_w and $\varepsilon_{polymer}$ are the permittivity of water and of the polymers (PNIPAM and PAA), respectively; f_w is the content of water in the microsphere. As temperature increases, the microspheres collapse and water molecules within the microspheres are expelled out continuously, resulting in a decrease in the permittivity ε_p of microspheres. Equation 9 also suggests that ε_p should be smaller than ε_w. However, Figure 6 shows that

DOI: 10.1021/acs.jpcb.5b05491
J. Phys. Chem. B 2015, 119, 13198−13207

Table 2. Phase Parameters of SIPN Microgel Solution with 10 wt % PAA (a) and 20 wt % PAA (b)[a]

(a) t/ °C	κ_a (mS·m^{-1})	Φ	ε_p	κ_p (mS·m^{-1})
25.8	2.8	0.57	89.9	7.2
28.0	3.0	0.45	92.5	9.2
30.2	3.2	0.41	91.2	10.3
33.8	3.5	0.31	90.4	14.2
36.2	3.7	0.21	93.9	28.9
39.2	3.8	0.19	94.5	38.4
40.5	3.9	0.2	92.2	35.8
44.0	4.1	0.22	87.8	27.3
48.2	4.5	0.22	83.9	25.7
52.3	4.8	0.24	81.6	23.3
(b) t/ °C	κ_a (mS·m^{-1})	Φ	ε_p	κ_p (mS·m^{-1})
27.2	0.9	0.66	78.2	2.0
30.0	0.9	0.66	75.1	2.0
33.5	1.0	0.60	79.0	2.3
36.4	1.2	0.41	67.8	2.9
39.0	1.3	0.38	67.0	3.0
41.0	1.4	0.33	64.4	3.2
44.0	1.5	0.31	61.4	3.4
47.6	1.6	0.30	61.2	3.3
50.8	1.7	0.29	59.2	3.3

[a]Notes: The data at T < VPTT are only for reference, because in this temperature range it is improper to explain the swollen microgel solution using interface polarization theory.

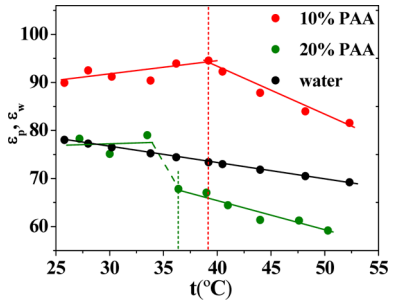

Figure 6. Temperature dependence of the permittivity of microgel particles and water (ε_p, ε_w).

$\varepsilon_{p(10\text{ wt \% PAA})}$ is greater than ε_w. This suggests that compared with microgel with more PAA, a special ordered arrangement of water molecules is formed in compacter microgel (with PAA 10 wt %) due to its weaker electrostatic repulsion. This is consistent with the findings of R. Allen,[50] V. Ballenegger,[51] and J. Marti[52] who advocated that water molecules in confined space will produce a large macroscopic dipole moment. This is an implication that the doping content of PAA has effects on the spatial structure of the microsphere network, leading to a different arrangement of water molecules and an evident distinction of ε_p. This kind of material with larger dielectric constant or polarity will produce a strong dipole−dipole interaction with drug molecules of larger polarity, which can lead to a higher loading capacity.[53]

As can be seen from Table 2, ϕ and ε_p decrease with temperature, suggesting a dehydration process. As T rises, water molecules are gradually expelled from SIPN microgels and carry part of the counterions into aqueous phase. This leads to the increase in solution conductivity κ_a. Meanwhile, κ_p increases with temperature, suggesting that, as the microgel collapses, the surface charge density is significantly increased. The analysis above proves that dielectric analysis combining the relaxation mechanism and the physical model is an innovative idea to study the volume phase transition of microgels.

3.3. High-Frequency Relaxation: The Structure Change of PAA Domain in the Phase Transition Process.

Although there is no covalent bond between the two networks in SIPN microgel, the conformational change of linear PAA chains as the microgel collapses is hardly unexpected. To reveal the change of PAA during the volume phase transition, the high-frequency relaxation was analyzed. We describe high-frequency relaxation with the model of counterion polarization,[54] i.e., the charged PAA spherical particles surrounded by a layer of counterions disperse in the continuous PNIPAM network medium and the counterions can move along the particles tangentially and radially, as shown in Figure 7. This

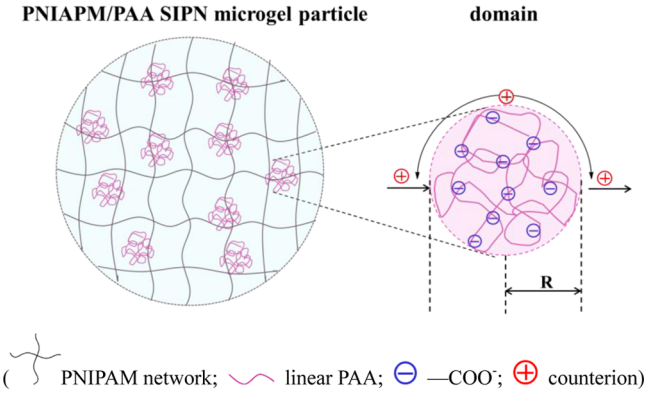

Figure 7. High-frequency relaxation mechanism schematic.

motion causes the high-frequency dielectric relaxation. The relation between the relaxation time τ_h and the characteristic migration length (domain radius R) is expressed as

$$\tau_h = \frac{R^2}{2D_{NH_4^+}} \quad (10)$$

where $D_{NH_4^+}$ is the diffusion coefficient of the counterion as defined previously.

Figure 8 shows that R (caculated by eq 10) reduces with temperature. This result clearly shows that the domain size

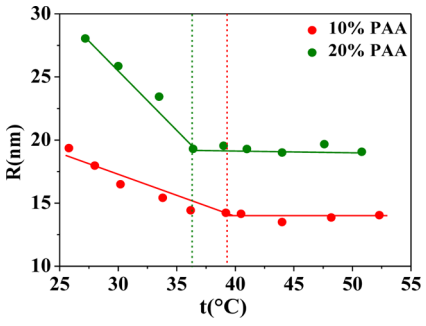

Figure 8. Temperature dependence of domain radius R.

formed by nonthermosensitive PAA also reduces with temperature. This suggests that the physical interaction between PAA and thermosensitive PNIPAM cannot be neglected. Besides, R twists at different temperature (VPTT), which indicates that

DOI: 10.1021/acs.jpcb.5b05491
J. Phys. Chem. B 2015, 119, 13198−13207

the interaction between them is closely related to the composition content in SIPN microgel.

Below VPTT, the decrease rate of R for SIPN microgel with 20 wt % PAA is noticeably faster than that of microgel with 10 wt % PAA. This shows that SIPN microgel with more PAA has better thermal response and swelling properties, which is of potential application as drug carrier material with higher loading capacity.[6] Interestingly, the domain size of SIPN microgel with more PAA is relatively larger, which can be explained by Donatelli's semiempirical quantitative formula[55]

$$D_2 = \frac{2\gamma W_2}{RT\nu_1\left[\left(\frac{1}{1-W_2}\right)^{2/3} + \frac{W_2}{\nu_1 M_2} - \frac{1}{2}\right]} \quad (11)$$

where D_2 is the domain size formed by polymer II (PAA in this work); ν_1 is the cross-linking density of polymer I (PNIPAM in this work); γ is the interfacial tension between the two polymers and the greater the miscibility, the smaller the value; W_2 and M_2 is the weight fraction and molecular weight of polymer II, respectively. It is easy to understand from eq 11 that the domain size R is inversely proportional to the cross-linking density of PNIPAM network. From this, we can deduce that the higher the content of PAA, the lower the content of PNIPAM, leading to a smaller cross-linking density: that is to say, the domain size is larger when there are more PAA in SIPN microgel, which is well supported by our dielectric analysis results shown in Figure 8.

3.4. Anomalous VPTT of SIPN Microgel. We have shown that different doping content of PAA leads to different VPTT. Further, we have also studied the dielectric behavior of pure PNIPAM microgels under the same condition. Figure 9 is the temperature dependence of permittivity at 14 kHz of pure PNIPAM and SIPN microgel. It is obvious that VPTT of them are different from each other: VPTT of PNIPAM is around 34 °C, which has been already confirmed by a large number of experiments,[56,57] including ours;[29] while SIPN microgels with 10 and 20 wt % PAA transform at 39 and 36 °C, respectively. According to the Flory−Rehner theory,[58] when gel reaches thermodynamic equilibrium, the free energy is from mixing free energy, elastic (or deformation) contribution, as well as the contribution from electrostatic effects. As the charged PAA is incorporated into the PNIPAM network, it needs to overcome electrostatic energy when phase transition occurs. This means that the contribution of the third term (electrostatic effects) is increased. As a result, the VPTT is significantly increased, i.e., the VPTT of SIPN is larger than that of PNIPAM. However, the VPTT of the SIPN microgel does not increase with PAA content as we expected. Conversely, the VPTT of SIPN microgel containing more PAA is lower than that with less PAA. From the perspective of interaction, this anomalous VPTT can be understood as follows.

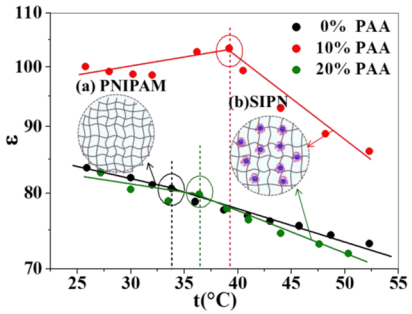

Figure 9. Temperature dependence of permittivity for PNIPAM/PAA SIPN microgel with different PAA contents at 14 kHz: (a) PNIPAM microgel (0 wt % PAA), (b) PNIPAM/PAA SIPN microgel (10 wt % PAA, 20 wt % PAA).

The phase transition of PNIPAM is actually a competition result of several intermolecular interactions:[7] H-bond interaction of PNIPAM-H_2O (facilitate dissolution) and hydrophobic interaction of PNIPAM pendent isopropyl groups as well as that of backbone (facilitate phase separation). Below VPTT, the H-bond interaction between PNIPAM and H_2O plays a dominant role; therefore, PNIPAM can swell in water at low temperatures. When temperature rises, H-bond interaction weakens and hydrophobic interaction dominates, which leads to phase separation. Thus, the polymer "solvation-phase separation" can be switched by enhancing one of these interactions or by weakening another.[59] After the incorporation of hydrophilic PAA chains, on one hand, the electrostatic repulsion between fixed charges −COO− makes the microgel difficult to collapse, while the doped PAA makes the microgel more hydrophilic, which to some extent increases VPTT; on the other hand, since PAA is partly protonated at the pH of this work, the H-bond between PNIPAM-PAA renders PNIPAM more hydrophobic, lowering VPTT.[60,61] The competition of these interactions eventually determines VPTT of the microgel.[62] This result provides the possibility for preparing thermosensitive materials with appropriate VPTT.

3.5. Thermodynamic Analysis of Relaxation Processes. The dielectric relaxation phenomenon can be viewed as the dipole rotation or ion migration between two equilibrium positions which are separated by a potential barrier. The relaxation time τ determined by a relaxation rate constant $k = 1/\tau$ depends on the height of the potential barrier. The height

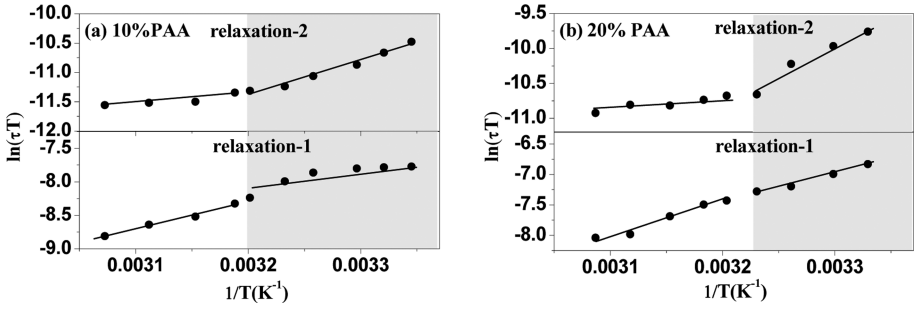

Figure 10. Eyring plots of relaxation time of low- and high-frequency relaxation of SIPN microgels with different contents of PAA: (a) 10 wt % PAA, (b) 20 wt % PAA.

DOI: 10.1021/acs.jpcb.5b05491
J. Phys. Chem. B 2015, 119, 13198−13207

is equal to the mole free activation energy of the relaxation processes, defined as $\Delta G = \Delta H - T\Delta S$. The thermodynamic parameters, ΔH and ΔS, are the enthalpy and entropy of activation for the relaxation process, respectively, and can be evaluated using Eyring's rate equation[63,64]

$$\ln \tau T = \ln\left(\frac{h}{k_B}\right) - \frac{\Delta S}{R} + \frac{\Delta H}{RT} \quad (12)$$

where h is the Planck's constant, and R and k_B represent the gas constant and Boltzmann constant, respectively.

Figure 10 shows the temperature dependence of $\ln \tau T$ versus $1/T$ of different SIPN microgel suspensions. Evidently, both the low- and high-relaxation processes show good linear relations between $\ln \tau T$ and $1/T$, but they are divided into two line segments around VPTT, i.e., they exhibit significant twists around VPTT. The corresponding thermodynamic parameters, ΔH and ΔS, for these relaxation processes below and above VPTT are obtained by the slopes and intercepts of these linear plots. The results are tabulated in Table 3.

Table 3. Thermodynamic Parameters Estimated from Eyring's Rate Equation for the SIPN Microgel with Different PAA Contents: (a) Low-Frequency Relaxation (b) High-Frequency Relaxation

	ΔS/J·K·mol^{-1}		ΔH/kJ·mol^{-1}	
(a) Content of PAA	T < VPTT	T > VPTT	T < VPTT	T > VPTT
10%	−50.4	−21.0	24.8	33.6
20%	−12.1	17.6	38.6	47.9
	ΔS/J·K·mol^{-1}		ΔH/kJ·mol^{-1}	
(b) Content of PAA	T < VPTT	T > VPTT	T < VPTT	T > VPTT
10%	55.4	−58.8	49.4	13.8
20%	126.8	−59.2	73.1	15.4

According to the thermal activation theory over potential barrier that describes temperature dependence of nearly all reaction rate processes,[64] the relaxation processes can be considered as the transfer of dipoles between two states: unpolarized state and polarized state as shown in Figure 11. By means of this double-well potential model, we can analyze the thermodynamic parameters summarized in Table 3 as follows.

1. For the micro-Brownian motion, which is dominant in the low-frequency relaxation below VPTT, $0 < \Delta H_{(10\%PAA)} < \Delta H_{(20\%PAA)}$ indicates that the solvated polymer segment needs to overcome an energy barrier of breaking the hydrogen bonds between H_2O and PNIPAM to be polarized, and the micro-Brownian motion of SIPN microgel with 20 wt % PAA is blocked more seriously, as there are more PAA chains entangled with PNIPAM. $\Delta S_{(10\%PAA)} < \Delta S_{(20\%PAA)} < 0$ suggests that the network tends to be orderly and the environment of the system with less PAA is more cooperative for the reorientation of the solvated polymer segment.

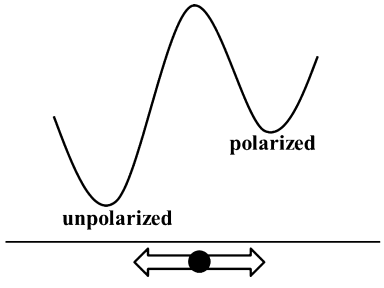

Figure 11. Concept of the double-well potential of the relaxation process (polarization process). The double lined arrow indicates the orientations of macroscopic dipole.

2. For the low-frequency relaxation above VPTT, the relaxation mechanism is from the diffusive motion of the counterion in the electric double layer (EDL) around the collapsed microspheres, interface polarization essentially. ΔH of the relaxation process depends on the Debye length. $0 < \Delta H_{(10\%PAA)} < \Delta H_{(20\%PAA)}$ indicates that counterions in microgel with 20 wt % PAA need to absorb more energy to move longer distance, verifying that the EDL of microgel with 20% PAA is thicker than that of 10% PAA. The entropy change tendency above VPTT is opposite: microgel suspension containing less PAA becomes ordered ($\Delta S_{10\%PAA} < 0$) above VPTT, while for microgel containing more PAA it becomes disordered ($\Delta S_{20\%PAA} > 0$). This indicates that a special ordered orientation is formed in the former system, which is contributed from directional orientation of water molecules as suggested in Section 3.2.3.

3. With regard to the high-frequency relaxation that originates from counterion polarization, the counterions need to overcome the electrostatic energy barriers between negatively charged carboxyl groups to migrate and redistribute. $\Delta H_{(10\%PAA)} < \Delta H_{(20\%PAA)}$ means that the counterions in microgel with 20% PAA need to absorb more energy to move longer distance, which is consistent with analytical results of high frequency relaxation (Figure 12). The value of ΔS is positive below VPTT and eventually becomes negative above VPTT. This implies that the range of motion of the counterions is limited above VPTT because the domain size reduces to a fixed value.

4. CONCLUSIONS

Dielectric behavior of PNIPAM/PAA SIPN microgel suspension composed of PNIPAM network and different contents of linear PAA (10 wt %, 20 wt %) was systematically studied in a frequency range from 40 Hz to 110 MHz as a function of temperature. After removing the effect of electrode polarization successfully, two relaxation processes were observed. The temperature dependence of the domain size obtained from high-frequency relaxation (counterions polarization) indicates that the nonthermosensitive PAA also decreases with temperature due to the synergistic effect of PNIPAM network, and that SIPN microgel with higher content of PAA has better thermal response and swelling property. The low-frequency relaxation is dominated by different relaxation mechanisms: the micro-Brownian motion of the solvated polymer segment below VPTT and interfacial polarization above VPTT. Phase parameters of collapsed microgels obtained by Hanai's approach show that permittivity of microgel with 10 wt % PAA is greater than that with 20 wt %. This suggests that an ordered structure of water molecules is formed in the limited space of the compacted microgel.

Compared with the pure PNIPAM microgel, we find that VPTT of SIPN microgel is significantly increased (0% PAA 34 °C, 10 wt % PAA 39 °C, 20 wt % PAA 36 °C). The experimentally anomalous VPTT is from a combined effect of electrostatic repulsion and hydrophilic/hydrophobic interaction, which depends on component contents. Dielectric measurements of the same systems as a function of temperature show that the change of entropy and enthalpy in relaxation

DOI: 10.1021/acs.jpcb.5b05491
J. Phys. Chem. B 2015, 119, 13198−13207

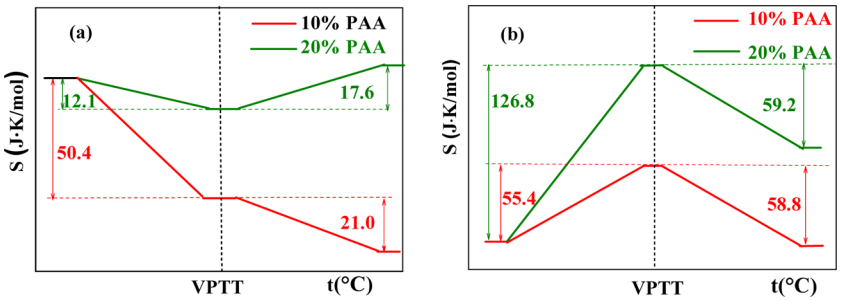

Figure 12. Entropy change diagram of microgel with different contents of PAA in the process of (a) low-frequency relaxation and (b) high-frequency relaxation.

processes provided us with valuable information on the micromechanism of the relaxations. This study throws light on understanding and regulating the volume phase transition behavior of complex polymers.

AUTHOR INFORMATION

Corresponding Author

*E-mail: zhaoks@bnu.edu.cn. Phone: +86-10-58805856.

Notes

The authors declare no competing financial interest.

ACKNOWLEDGMENTS

The authors would like to thank Prof. Guanghui Ma and Dr. Enping Lai of Institute of Process Engineering, Chinese Academy of Science for supplying the sample used in this work. The financial support from the National Natural Scientific Foundation of China (No. 21173025, 21473012) and the Major Research Plan of NSFC (No. 21233003) are gratefully acknowledged.

REFERENCES

(1) Hiruta, Y.; Shimamura, M.; Matsuura, M.; Maekawa, Y.; Funatsu, T.; Suzuki, Y.; Ayano, E.; Okano, T.; Kanazawa, H. Temperature-Responsive Fluorescence Polymer Probes with Accurate Thermally Controlled Cellular Uptakes. *ACS Macro Lett.* **2014**, *3*, 281−285.

(2) Strong, L. E.; Dahotre, S. N.; West, J. L. Hydrogel-Nanoparticle Composites for Optically Modulated Cancer Therapeutic Delivery. *J. Controlled Release* **2014**, *178*, 63−68.

(3) Gupta, M. K.; Martin, J. R.; Werfel, T. A.; Shen, T.; Page, J. M.; Duvall, C. L. Cell Protective, Abc Triblock Polymer-Based Thermoresponsive Hydrogels with Ros-Triggered Degradation and Drug Release. *J. Am. Chem. Soc.* **2014**, *136*, 14896−14902.

(4) Sambe, L.; de La Rosa, V. R.; Belal, K.; Stoffelbach, F.; Lyskawa, J.; Delattre, F.; Bria, M.; Cooke, G.; Hoogenboom, R.; Woisel, P. Programmable Polymer- Based Supramolecular Temperature Sensor with a Memory Function**. *Angew. Chem., Int. Ed.* **2014**, *53*, 5044−5048.

(5) Yu, Q.; Johnson, L. M.; Lopez, G. P. Nanopatterned Polymer Brushes for Triggered Detachment of Anchorage-Dependent Cells. *Adv. Funct. Mater.* **2014**, *24*, 3751−3759.

(6) Chen, Y.; Ding, D.; Mao, Z.; He, Y.; Hu, Y.; Wu, W.; Jiang, X. Synthesis of Hydroxypropylcellulose-Poly(Acrylic Acid) Particles with Semi-Interpenetrating Polymer Network Structure. *Biomacromolecules* **2008**, *9*, 2609−2614.

(7) Ilmain, F.; Tanaka, T.; Kokufuta, E. Volume Transition in a Gel Driven by Hydrogen Bonding. *Nature* **1991**, *349*, 400−401.

(8) Xing, Z. M.; Wang, C. L.; Yan, J.; Zhang, L.; Li, L.; Zha, L. S. Dual Stimuli Responsive Hollow Nanogels with Ipn Structure for Temperature Controlling Drug Loading and Ph Triggering Drug Release. *Soft Matter* **2011**, *7*, 7992−7997.

(9) Liu, X. Y.; Guo, H.; Zha, L. S. Study of Ph/Temperature Dual Stimuli-Responsive Nanogels with Interpenetrating Polymer Network Structure. *Polym. Int.* **2012**, *61*, 1144−1150.

(10) Zhou, J.; Wang, G.; Zou, L.; Tang, L.; Marquez, M.; Hu, Z. Viscoelastic Behavior and in Vivo Release Study of Microgel Dispersions with Inverse Thermoreversible Gelation. *Biomacromolecules* **2008**, *9*, 142−148.

(11) Xia, X.; Hu, Z. Synthesis and Light Scattering Study of Microgels with Interpenetrating Polymer Networks. *Langmuir* **2004**, *20*, 2094−2098.

(12) Hu, Z.; Xia, X. Hydrogel Nanoparticle Dispersions with Inverse Thermoreversible Gelation. *Adv. Mater.* **2004**, *16*, 305−309.

(13) Stile, R. A.; Healy, K. E. Poly(*N*-Isopropylacrylamide)-Based Semi-Interpenetrating Polymer Networks for Tissue Engineering Applications. 1. Effects of Linear Poly(Acrylic Acid) Chains on Phase Behavior. *Biomacromolecules* **2002**, *3*, 591−600.

(14) Kozhunova, E. Y.; Makhaeva, E. E.; Khokhlov, A. R. Collapse of Thermosensitive Polyelectrolyte Semi-Interpenetrating Networks. *Polymer* **2012**, *53*, 2379−2384.

(15) Zhang, B.; Sun, S.; Wu, P. Synthesis and Unusual Volume Phase Transition Behavior of Poly(*N*-Isopropylacrylamide)-Poly(2-Hydroxyethyl Methacrylate) Interpenetrating Polymer Network Microgel. *Soft Matter* **2013**, *9*, 1678−1684.

(16) Zhang, B.; Tang, H.; Wu, P. The Unusual Volume Phase Transition Behavior of the Poly(*N*-Isopropylacrylamide)-Poly(2-Hydroxyethyl Methacrylate) Interpenetrating Polymer Network Microgel: Different Roles in Different Stages. *Polym. Chem.* **2014**, *5*, 5967−5977.

(17) Tominaga, T.; Tirumala, V. R.; Lee, S.; Lin, E. K.; Gong, J. P.; Wu, W.-l. Thermodynamic Interactions in Double-Network Hydrogels. *J. Phys. Chem. B* **2008**, *112*, 3903−3909.

(18) Šťastná, J.; Hanyková, L.; Sedláková, Z.; Valentová, H.; Spěváček, J. Temperature-Induced Phase Transition in Hydrogels of Interpenetrating Networks Poly (*N*-Isopropylmethacrylamide)/Poly (*N*-Isopropylacrylamide). *Colloid Polym. Sci.* **2013**, *291*, 2409−2417.

(19) Sun, S.; Hu, J.; Tang, H.; Wu, P. Chain Collapse and Revival Thermodynamics of Poly (*N*-Isopropylacrylamide) Hydrogel. *J. Phys. Chem. B* **2010**, *114*, 9761−9770.

(20) Lai, H.; Wu, P. A Infrared Spectroscopic Study on the Mechanism of Temperature-Induced Phase Transition of Concentrated Aqueous Solutions of Poly (*N*-Isopropylacrylamide) and *N*-Isopropylpropionamide. *Polymer* **2010**, *51*, 1404−1412.

(21) Ono, Y.; Shikata, T. Hydration and Dynamic Behavior of Poly (*N*-Isopropylacrylamide) S in Aqueous Solution: A Sharp Phase Transition at the Lower Critical Solution Temperature. *J. Am. Chem. Soc.* **2006**, *128*, 10030−10031.

(22) Ono, Y.; Shikata, T. Contrary Hydration Behavior of *N*-Isopropylacrylamide to Its Polymer, P (Nipam), with a Lower Critical Solution Temperature. *J. Phys. Chem. B* **2007**, *111*, 1511−1513.

(23) Nakano, S.; Sato, Y.; Kita, R.; Shinyashiki, N.; Yagihara, S.; Sudo, S.; Yoneyama, M. Molecular Dynamics of Poly (*N*-Isopropylacrylamide) in Protic and Aprotic Solvents Studied by Dielectric Relaxation Spectroscopy. *J. Phys. Chem. B* **2012**, *116*, 775−781.

DOI: 10.1021/acs.jpcb.5b05491
J. Phys. Chem. B 2015, 119, 13198−13207

(24) Füllbrandt, M.; von Klitzing, R.; Schönhals, A. Probing the Phase Transition of Aqueous Solutions of Linear Low Molecular Weight Poly (*N*-Isopropylacrylamide) by Dielectric Spectroscopy. *Soft Matter* **2012**, *8*, 12116−12123.
(25) Füllbrandt, M.; von Klitzing, R.; Schönhals, A. The Dielectric Signature of Poly (*N*-Isopropylacrylamide) Microgels at the Volume Phase Transition: Dependence on the Crosslinking Density. *Soft Matter* **2013**, *9*, 4464−4471.
(26) Füllbrandt, M.; Ermilova, E.; Asadujjaman, A.; Hölzel, R.; Bier, F. F.; von Klitzing, R.; Schönhals, A. Dynamics of Linear Poly(*N*-Isopropylacrylamide) in Water around the Phase Transition Investigated by Dielectric Relaxation Spectroscopy. *J. Phys. Chem. B* **2014**, *118*, 3750−3759.
(27) Gómez-Galván, F.; Lara-Ceniceros, T.; Mercado-Uribe, H. Device for Simultaneous Measurements of the Optical and Dielectric Properties of Hydrogels. *Meas. Sci. Technol.* **2012**, *23*, 025602.
(28) Zhou, J. F.; Wei, J. J.; Ngai, T.; Wang, L.; Zhu, D.; Shen, J. Correlation between Dielectric/Electric Properties and Cross-Linking/Charge Density Distributions of Thermally Sensitive Spherical Pnipam Microgels. *Macromolecules* **2012**, *45*, 6158−6167.
(29) Su, W.; Zhao, K.; Wei, J.; Ngai, T. Dielectric Relaxations of Poly(*N*-Isopropylacrylamide) Microgels near the Volume Phase Transition Temperature: Impact of Cross-Linking Density Distribution on the Volume Phase Transition. *Soft Matter* **2014**, *10*, 8711−8723.
(30) Wang, Y.; Qin, J.; Wei, Y.; Li, C.; Ma, G. Preparation Strategies of Thermo-Sensitive P(Nipam-Co-Aa) Microspheres with Narrow Size Distribution. *Powder Technol.* **2013**, *236*, 107−113.
(31) Si, T.; Wang, Y.; Wei, W.; Lv, P.; Ma, G.; Su, Z. Effect of Acrylic Acid Weight Percentage on the Pore Size in Poly(*N*-Isopropyl Acrylamide-Co-Acrylic Acid) Microspheres. *React. Funct. Polym.* **2011**, *71*, 728−735.
(32) Wei, Y.; Wang, Y.-X.; Wang, W.; Ho, S. V.; Wei, W.; Ma, G.-H. Mpeg-Pla Microspheres with Narrow Size Distribution Increase the Controlled Release Effect of Recombinant Human Growth Hormone. *J. Mater. Chem.* **2011**, *21*, 12691−12699.
(33) Sperling, L.; Hu, R. Interpenetrating Polymer Networks. In *Polymer Blends Handbook*; Springer, 2014; pp 677−724.
(34) Sperling, L. H. History of Interpenetrating Polymer Networks Starting with Bakelite-Based Compositions. In *100+ Years of Plastics. Leo Baekeland and Beyond*; American Chemical Society: 2011; Vol. *1080*, pp 69−82.
(35) Lipatov, Y. S.; Alekseeva, T. T. *Phase-Separated Interpenetrating Polymer Networks*; Springer: 2007.
(36) Schwan, H. Determination of Biological Impedances. In *Physical Techniques in Biological Research*; Academic Press: New York, 1963; p 323.
(37) Serghei, A.; Tress, M.; Sangoro, J.; Kremer, F. Electrode Polarization and Charge Transport at Solid Interfaces. *Phys. Rev. B: Condens. Matter Mater. Phys.* **2009**, *80*, 184301.
(38) Havriliak, S.; Negami, S. A Complex Plane Representation of Dielectric and Mechanical Relaxation Processes in Some Polymers. *Polymer* **1967**, *8*, 161−205 appendix 206−10.
(39) Steeman, P. A. M.; van Turnhout, J. Fine Structure in the Parameters of Dielectric and Viscoelastic Relaxations. *Macromolecules* **1994**, *27*, 5421−7.
(40) Wübbenhorst, M.; van Turnhout, J. "Conduction - Free" Dielectric Loss De/Dlnf - a Powerful Tool for the Analysis of Strong (Ion) Conducting Dielectric Materials. *Dielectrics Newsletter*, 2000
(41) Jiménez, M.; Arroyo, F.; van Turnhout, J.; Delgado, A. Analysis of the Dielectric Permittivity of Suspensions by Means of the Logarithmic Derivative of Its Real Part. *J. Colloid Interface Sci.* **2002**, *249*, 327−335.
(42) Wübbenhorst, M.; van Turnhout, J. Analysis of Complex Dielectric Spectra. I. One-Dimensional Derivative Techniques and Three-Dimensional Modelling. *J. Non-Cryst. Solids* **2002**, *305*, 40−49.
(43) Jimenez, M. L.; Arroyo, F. J.; Carrique, F.; Kaatze, U. Broadband Dielectric Spectra of Spheroidal Hematite Particles. *J. Phys. Chem. B* **2003**, *107*, 12192−12200.
(44) Dukhin, S. Electrochemical Characterization of the Surface of a Small Particle and Nonequilibrium Electric Surface Phenomena. *Adv. Colloid Interface Sci.* **1995**, *61*, 17−49.
(45) Lide, D. R. *2001, CRC Handbook of Chemistry and Physics*; CRC Press: Boca Raton, FL, 2000.
(46) Hanai, T. Theory of the Dielectric Dispersion Due to the Interfacial Polarization and Its Application to Emulsions. *Colloid Polym. Sci.* **1960**, *171*, 23−31.
(47) Zhao, K.; Asami, K.; Lei, J. Dielectric Analysis of Chitosan Microsphere Suspensions: Study on Its Ion Adsorption. *Colloid Polym. Sci.* **2002**, *280*, 1038−1044.
(48) Wang, J.; Zhao, K.; Zhang, L. Dielectric Analysis of Tio2-Based Electrorheological Suspensions. *Rheol. Acta* **2013**, *52*, 115−125.
(49) Fan, X.; Zhao, K. Aggregation Behavior and Electrical Properties of Amphiphilic Pyrrole-Tailed Ionic Liquids in Water, from the Viewpoint of Dielectric Relaxation Spectroscopy. *Soft Matter* **2014**, *10*, 3259−3270.
(50) Allen, R.; Hansen, J.-P. Electrostatic Interactions of Charges and Dipoles near a Polarizable Membrane. *Mol. Phys.* **2003**, *101*, 1575−1585.
(51) Ballenegger, V.; Hansen, J.-P. Dielectric Permittivity Profiles of Confined Polar Fluids. *J. Chem. Phys.* **2005**, *122*, 114711.
(52) Martí, J.; Nagy, G.; Guàrdia, E.; Gordillo, M. C. Molecular Dynamics Simulation of Liquid Water Confined inside Graphite Channels: Dielectric and Dynamical Properties. *J. Phys. Chem. B* **2006**, *110*, 23987−23994.
(53) Shah, J. C.; Sadhale, Y.; Chilukuri, D. M. Cubic Phase Gels as Drug Delivery Systems. *Adv. Drug Delivery Rev.* **2001**, *47*, 229−250.
(54) O'Brien, R. W. The High-Frequency Dielectric Dispersion of a Colloid. *J. Colloid Interface Sci.* **1986**, *113*, 81−93.
(55) Donatelli, A.; Sperling, L.; Thomas, D. A Semiempirical Derivation of Phase Domain Size in Interpenetrating Polymer Networks. *J. Appl. Polym. Sci.* **1977**, *21*, 1189−1197.
(56) Heskins, M.; Guillet, J. E. Solution Properties of Poly (*N*-Isopropylacrylamide). *J. Macromol. Sci., Chem.* **1968**, *2*, 1441−1455.
(57) Fujishige, S.; Kubota, K.; Ando, I. Phase Transition of Aqueous Solutions of Poly (*N*-Isopropylacrylamide) and Poly (*N*-Isopropylmethacrylamide). *J. Phys. Chem.* **1989**, *93*, 3311−3313.
(58) Quesada-Pérez, M.; Maroto-Centeno, J. A.; Forcada, J.; Hidalgo-Alvarez, R. Gel Swelling Theories: The Classical Formalism and Recent Approaches. *Soft Matter* **2011**, *7*, 10536−10547.
(59) Nayak, S.; Lyon, L. A. Soft Nanotechnology with Soft Nanoparticles. *Angew. Chem., Int. Ed.* **2005**, *44*, 7686−7708; *Angew. Chem.* **2005**, *117*, 7862−7886.
(60) Chen, G.; Hoffman, A. S. Graft Copolymers That Exhibit Temperature-Induced Phase Transitions over a Wide Range of Ph. *Nature* **1995**, *373*, 49−52.
(61) Shin, B. C.; Jhon, M. S.; Lee, H. B.; Yuk, S. H. Ph/Temperature Dependent Phase Transition of an Interpenetrating Polymer Network: Anomalous Swelling Behavior above Lower Critical Solution Temperature. *Eur. Polym. J.* **1998**, *34*, 1675−1681.
(62) Kelmanovich, S. G.; Parke-Houben, R.; Frank, C. W. Competitive Swelling Forces and Interpolymer Complexation in Ph- and Temperature-Sensitive Interpenetrating Network Hydrogels. *Soft Matter* **2012**, *8*, 8137−8148.
(63) Smith, G.; Shekunov, B.; Shen, J.; Duffy, A.; Anwar, J.; Wakerly, M.; Chakrabarti, R. Dielectric Analysis of Phosphorylcholine Head Group Mobility in Egg Lecithin Liposomes. *Pharm. Res.* **1996**, *13*, 1181−1185.
(64) Blythe, T.; Bloor, D. *Electrical Properties of Polymers*, 2nd ed.; Cambridge University Press: New York, 2005; pp 66−69.

DOI: 10.1021/acs.jpcb.5b05491
J. Phys. Chem. B 2015, 119, 13198−13207